

## **INFLUENCE OF BIMOMENT RESTRAINTS ON THE LOAD-BEARING CAPACITY OF A STEEL I-BEAM**

Krzysztof WIERZBICKI<sup>1</sup>

Faculty of Civil and Environmental Engineering, West Pomeranian University of  
Technology, Szczecin, Poland

### **A b s t r a c t**

The study presents an analysis of steel I-beam warping. The calculations were made for hot-rolled IPE200 hinged beams with different lengths. After determining load-bearing capacity using the GMNIA method, the beams were strengthened with bimoment restraints at each end. The changes in critical moment and load-bearing capacity were then evaluated. The study presents the manner in which the material and geometric imperfections have been determined. The GMNIA calculations were conducted using the Finite Element Method in Abaqus software. The results were then compared to results obtained with traditional methods and acquired from LT Beam software.

Keywords: warping, lateral-torsional buckling, imperfections, stiffeners, bending, GMNIA

### **1. INTRODUCTION**

Steel I-beams are often used for the construction of bending elements in structures. In the case of beams that are not supported transversely to their longitudinal axis, their load-bearing capacity is often regarded in terms of the occurring warping. This phenomenon occurs when the stiffness of the element in the plane perpendicular to the bending plane is relatively small compared to the stiffness in the bending plane, which is a clear case in most I-beams. The result is buckling of

---

<sup>1</sup> Corresponding author: Faculty of Civil Engineering and Architecture, West Pomeranian University of Technology, al. Piastów 17, 70-310 Szczecin, Poland, e-mail: kwierzbicki@zut.edu.pl

the compressed flange, which rotates along the longitudinal axis of the element. Buckling is strictly correlated to changes in the shape which results in an uneven bending. It is also visible as warping of opposite flanges in their planes.

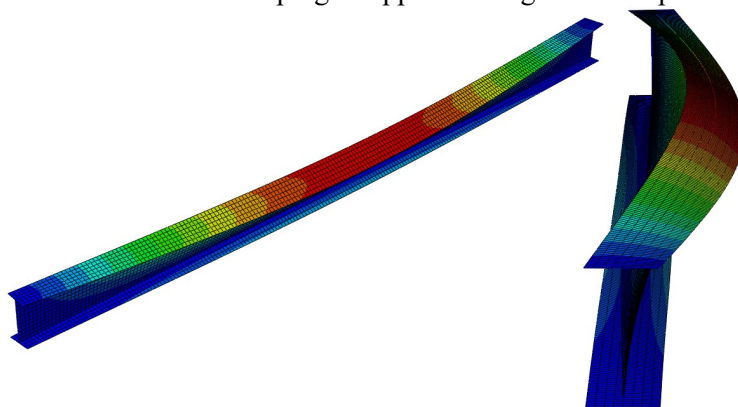


Fig. 1. Warping of the I-beam with a fork support and distributed downward load

Warping is affected by numerous factors and physical variables, the most important of which include geometric characteristics such as moment of inertia and total length. Of great significance are the boundary conditions of supports, which should, besides typical displacement and deviation from flatness, include deviation from the plane. In the case of a single dimension beam located in a three-dimensional space, there are three degrees of freedom for displacement perpendicular to each other, and three directions of rotation along those axes. One should also consider the seventh degree of freedom – warping of the section.

Another factor that influences warping is the type and location of load application. In case of a downward load applied to the upper flange, the load-bearing capacity reserves will be used to a higher degree than in case of load suspended from the bottom flange. Additionally, application of loads outside the axis of the web will impose torsion, which negatively affects the load-bearing capacity.

As warping can significantly limit the load-bearing capacity, the lateral-torsional resistance of beams is secured from loss of stability by side supports or the introduction of restraints and endplates. The effect of additional restraints is, however, only considered in estimates as more detailed analysis is non-existent in the prevailing standards. Their calculations are also time-consuming, which limits their use in practical engineering.

## 2. LITERATURE REVIEW

The maximum value of bending moment, which is transferred by an ideally elastic beam without any imperfections is called a critical moment ( $M_{cr}$ ). Standards in

force for the design of steel structures [1] do not provide a method for determining its value. However, methods for calculating the critical moment known as a “General Formula” can be found in Eurocode’s pre-standard [2] or other standards [3]:

$$M_{cr} = C_1 \frac{\pi^2 \cdot E \cdot I_z}{(k_z \cdot L)^2} \left( \sqrt{\left(\frac{k_z}{k_w}\right)^2 \frac{I_w}{I_z} + \frac{(k_z \cdot L)^2 \cdot G \cdot I_T}{\pi^2 \cdot E \cdot I_z} + (C_2 \cdot z_g - C_3 \cdot z_j)^2} - C_2 \cdot z_g - C_3 \cdot z_j \right) \quad (2.1)$$

where:

$M_{cr}$  – the critical moment of bending,

$C_1, C_2, C_3$  – factors depending on the loading and end restraint conditions,

$k_z$  – the effective length factor of lateral bending,

$k_w$  – the effective length factor of warping,

$E$  – Young’s modulus,

$G$  – the shear modulus,

$L$  – the length of the beam,

$I_w$  – the warping constant,

$I_T$  – the torsion constant,

$I_z$  – the second moment of area about the weak axis,

$z_g$  – the distance between the point of load application and the shear centre about the strong axis,

$z_j$  – the distance between the point of load application and the shear centre about the weak axis.

Additional non-dimensional factors such as  $C_1, C_2, C_3$ , or  $k_z$  and  $k_w$  are introduced as there is no simple calculation of critical moment for a simply-supported beam with non-fork support or non-centre alignment of external load. The general differential equation can be solved using a trial and error method [4] or approximated using, e.g., Laplace transformation [5].

Factor  $k_z$  and  $k_w$  take values from 0.5 to 1.0 (where 0.5 means full fixation on both supports and 1.0 means full pinned support). There is no description for the General Formula or in the European Standards regarding what element (e.g. endplate or stiffener) should be taken to assure full fixation or other value, e.g.,  $k_w=0.75$ .

The abovementioned concern about the determination of the critical moment value and other issues regarding, e.g., classification of steel channels based on their  $h/b$  ratio, makes the determination of load-bearing capacity of bending with warping included one of the most controversial aspects of European standards for designing steel structures [6].

Different approaches have been proposed by scientists as to how to determine the load-bearing capacity with warping included. One such approach is to condition

it from equivalent geometrical imperfections based on the Ayrton-Perry formula found in [7], which allows you to derive alternative buckling curves [8,9]

The analysis of the warping of steel channels is conducted mostly based on the Finite Element Method (FEM) in ABAQUS or ANSYS software. It is possible to use geometrically and materially nonlinear analysis with imperfections included (GMNIA) which allows reading out the load-bearing capacity straight from the results of the analysis as, e.g., a maximum force introduced to the model. In this type of analysis used to calculate the warping or buckling instead of typical initial geometrical imperfections [1] introduced by, e.g., additional loads, one can use the bend curvature corresponding to buckling form and scale it to the initial size of the imperfection [10]. It is then applied to the nodes of the model to impose initial buckling, which is then considered as the initial state.

There are two major methods of introducing initial imperfections to the model [11]. The first one replaces the initial imperfections with a known side-bend range according to, e.g., the Maquoi-Rondala proposal. The second one introduces the material imperfections resulting from residual stresses occurring in the production process (e.g. after rolling or welding) separately. The material imperfections can also occur due to the manufacturing tolerances of hot-rolled [12] and welded [13] elements. This study focuses on the former method.

One element that can limit warping in bent steel elements is the endplates as they allow connecting of two adjacent elements, and so, often they are necessary for designed structures. During the dimensioning of steel structures, the endplates are often excluded in the calculations even though they have a beneficial influence on the load-bearing capacity. The approximating formulas for determination of stiffness of endplates, which allows them to be included in the “General Formula”, can be found in [11,12]:

$$k_w = \mu_\omega = 0.5 + 0.14(\kappa_{\omega,1} + \kappa_{\omega,2}) + 0.055(\kappa_{\omega,1} + \kappa_{\omega,2})^2 \quad (2.2)$$

$$\kappa_\omega = \frac{1}{1 + \frac{s_{\omega,ini}L}{2EI_\omega}} \quad (2.3)$$

where:

$s_{\omega,ini}$  – the stiffness of an endplate,

$\kappa_\omega$  – the coefficient of the stiffness of fixations on both ends,

$\kappa_{\omega,1}, \kappa_{\omega,2}$  – the coefficients of the stiffness of fixation - respectively in the left and right support,

$E, I_\omega$  – as previous.

Such equations provide a solution for obtaining an exact value of the  $k_w$  factor using Saint Venant's stiffness of endplates. Unfortunately, the formulas can only be applied for the most common static schemes like a simply-supported I-beam under evenly distributed load.

Previously performed calculations [14] have proven that in order to significantly increase the I-beam load-bearing capacity by introduction of endplates, their thickness must often be bigger than the thickness of the web or even the flanges they will be welded to. This causes welding execution errors (thicker plate will have higher heat accumulation, meaning it should be initially heated before welding, resulting in increased welding stresses). To limit the thickness of the strengthening plates, instead of endplates, different types of stiffeners can be implemented. To those, we can include transverse ribs along the length of the beam, the X-shaped spacer, closed steel diaphragms, or bimoment restraints [5,15]. This study focuses on the latter of the aforementioned solutions.

In compliance with [15, 16, 17] and previous calculations, in simply-supported beams, the bimoment restraints and other warping restraints are the most effective when installed in the warping plane at the very ends, near the supports. According to the experiment conducted in [5], despite welding, there is always a risk of insufficient stiffness of the connection of the bimoment restraints. Thus, it cannot be considered as fully stiff.

### 3. MATERIALS AND METHOD

#### 3.1 Geometrical and material properties of the beam

A hot-rolled steel I-beam IPE200 of three different lengths – 4.5 m, 6.0 m, and 7.5 m was taken into consideration (Figure 2). The beams are simply- and fork-supported on both ends and in class 1 for bending.

The load is applied as a concentrated force in the middle of the span at the top flange (in the plane of the web). To increase the load-bearing capacity of bending, four longitudinal stiffeners were rigidly connected to the inner side of the flanges. The dimensions of each plate are 183 mm x 183 mm, with a thickness of between 5 and 50 mm.

As seen in Figure 3, the longitudinal stiffeners were installed where the highest rotation of the top and bottom flange occurs during warping.

For the purpose of calculations, the beams were assumed as S355JR with a bilinear operation model and no additional strengthening mechanism after the yield point (figure 4).

### 3.2 Methods

The calculations were conducted using the ABAQUS CAE environment in two stages:

**Stage 1:** The influence of size and type of elements mesh on the results acquired in Buckle analysis was determined. Three different lengths of the IPE200 I-beam were considered: 4.5 m, 6.0 m, and 7.5 m, without additional stiffeners. Restraints and loads are presented in Figure 2. Based on the acquired results, the type and size of the finite element was chosen. The element's properties were chosen as a middle ground between the precision of results and calculation time.

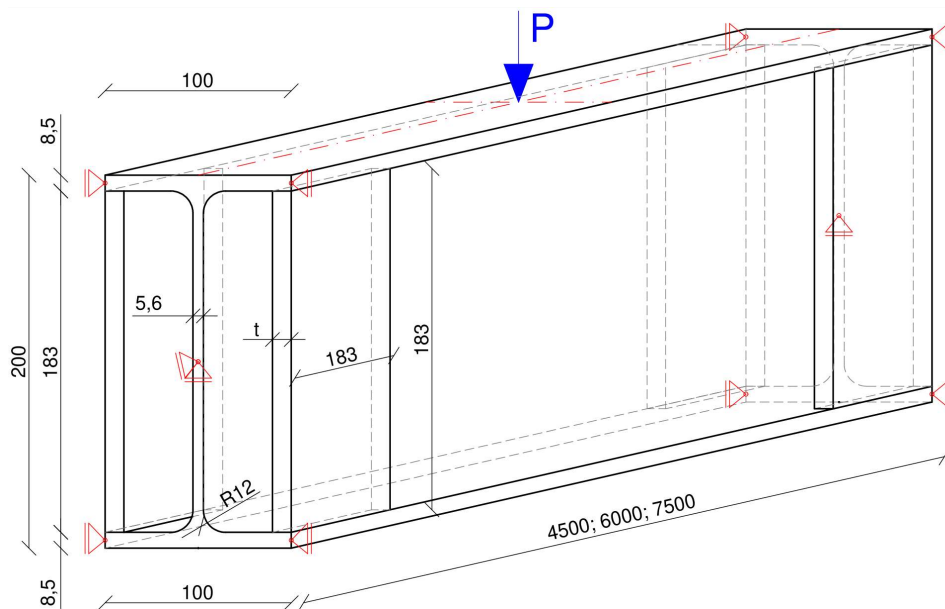


Fig. 2. Geometry of a reference beam,  $t$  – thickness of the stiffeners (from 5 to 50 mm); dimensions in millimetres

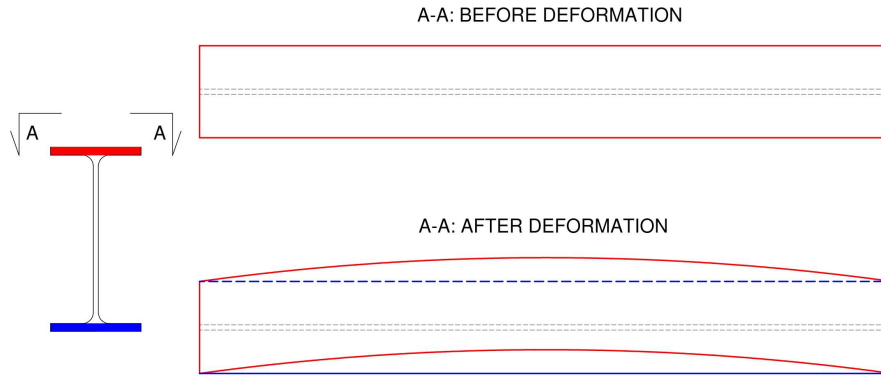


Fig. 3. Mutual rotation of flanges before and after LTB for a beam without stiffeners

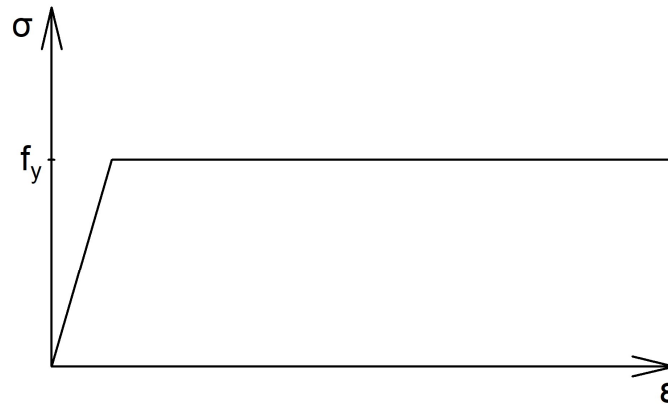


Fig. 4. Stress-strain correlation applied FEM model

**Stage 2:** The load-bearing capacity of bending was determined using the ABAQUS environment. For the purpose of the calculations, an initial equivalent imperfection was introduced [18]. Using the Riks method of incremental analysis, the loads were progressively increased until reaching load-bearing capacity at loss of stability or yield (whichever occurs faster). The calculations were conducted for different plate thickness of 5 mm to 50 mm and infinitely rigid IPE200 beams with lengths of 4.5 m, 6.0 m, and 7.5 m, respectively.

This approach allows you to perform the analysis including non-linear geometrical and material imperfections (GMNIA) which further allows you to acquire a direct value from the results. For the purpose of the second stage, an initial imperfection needs to be assumed. The value of the imperfection was calculated based on [18]:

$$e_{0,d} = \alpha_{LT}(\bar{\lambda}_{LT} - 0.2) \frac{M_{Rk}}{N_{Rk}} \quad (3.1)$$

where:

$\alpha_{LT}$  – imperfection factor, for  $h/b > 1.2$ :

$$\alpha_{LT} = 0.12\sqrt{W_{el,y}/W_{el,z}} \leq 0.34 \quad (3.2)$$

$W_{el,y}$  – first moment of area about the weak axis,

$W_{el,z}$  – first moment of area about the strong axis,

$\bar{\lambda}_{LT}$  – relative slenderness in bending according to [1],

$M_{Rk}$  – characteristic value of plastic load-bearing capacity of bending for cross-section about y-axis,

$N_{Rk}$  – characteristic value of load-bearing capacity of tension for a cross-section.

## 4. RESULTS AND DISCUSSION

### 4.1. Determination of elastic critical moment

As seen in Tables 2 and 3, the values of the critical moment obtained from the mesh models B20OS, C3D20, and S4 are similar. Different values have been obtained for the C3D8 model with 20 mm mesh.

Table 1. Values of  $M_{cr}$  for the calculations including volumetric mesh

| C3D20           |                   |             |           | C3D8            |                   |             |           |
|-----------------|-------------------|-------------|-----------|-----------------|-------------------|-------------|-----------|
| FE size<br>[mm] | $M_{cr}$<br>[kNm] | time<br>[s] | equations | FE size<br>[mm] | $M_{cr}$<br>[kNm] | time<br>[s] | equations |
| 5               | 24,83             | 2216        | 3040239   | 5               | 25,03             | 194         | 832293    |
| 10              | 24,94             | 197         | 625350    | 10              | 25,24             | 52          | 174891    |
| 20              | 25,11             | 62          | 176823    | 20              | 27,29             | 33          | 49665     |
| 30              | 25,16             | 39          | 74667     | 30              | 27,94             | 29          | 21105     |
| 40              | 25,35             | 35          | 46119     | 40              | 29,80             | 27          | 13137     |
| 50              | 25,36             | 33          | 36939     | 50              | 30,79             | 27          | 10527     |
| 60              | 25,36             | 33          | 30819     | 60              | 31,62             | 27          | 8787      |
| 70              | 25,57             | 33          | 20811     | 70              | 33,60             | 27          | 6003      |
| 80              | 25,92             | 31          | 18411     | 80              | 43,17             | 27          | 5313      |
| 90              | 25,93             | 29          | 16011     | 90              | 45,18             | 27          | 4623      |
| 100             | 25,93             | 29          | 14571     | 100             | 46,82             | 27          | 4209      |

Table 2. Results of  $M_{cr}$  for the calculations including surface and linear meshes

| <b>S4</b>       |                   |             |           | <b>B32OS</b>    |                   |             |           |
|-----------------|-------------------|-------------|-----------|-----------------|-------------------|-------------|-----------|
| FE size<br>[mm] | $M_{cr}$<br>[kNm] | time<br>[s] | equations | FE size<br>[mm] | $M_{cr}$<br>[kNm] | time<br>[s] | equations |
| 5               | 24,66             | 2216        | 3040239   | 5               | 25,18             | 35          | 66234     |
| 10              | 24,73             | 197         | 625350    | 10              | 25,25             | 27          | 8407      |
| 20              | 24,83             | 62          | 176823    | 20              | 25,25             | 27          | 4207      |
| 30              | 24,93             | 39          | 74667     | 30              | 25,25             | 27          | 2807      |
| 40              | 25,09             | 35          | 46119     | 40              | 25,25             | 27          | 2107      |
| 50              | 25,10             | 33          | 36939     | 50              | 25,25             | 27          | 1687      |
| 60              | 25,11             | 33          | 30819     | 60              | 25,25             | 27          | 1407      |
| 70              | 25,18             | 33          | 20811     | 70              | 25,25             | 27          | 1211      |
| 80              | 25,20             | 31          | 18411     | 80              | 25,25             | 27          | 1057      |
| 90              | 25,21             | 29          | 16011     | 90              | 25,25             | 27          | 931       |
| 100             | 25,22             | 29          | 14571     | 100             | 25,25             | 27          | 847       |

The results are affected by the shape of the finite elements, particularly those located on the web. The rather small thickness causes that with the increase in transverse mesh size the dimensions of the nodes differ greatly (e.g. a thickness of the element of 5.6 mm corresponds to the size of 50 mm for other two volumetric dimensions). The Finite Element Method which uses linear shape function for the determination of the polygons (included in B32OS, C3D8, and S4) gives the best results if the dimensions of the finite elements are similar. In the case of linear and shell elements, their thickness is not defined with geometrical nodes, but rather by attributing adequate stiffness. This does not allow the nodes to “stretch” on thin elements. Results for C3D8 are similar to those acquired for C3D20 and S4, where the smallest size of finite elements was used, which concurs with other studies [19]. Results for C3D8 would have been closer to other results if the web had a bigger thickness or higher mesh density. However, assuming a different mesh density for different models would result in bias in any comparison of those models.

Table 3. Relationship between length of the IPE200 beam and  $M_{cr}$  without stiffeners [kNm]

| Length<br>[m] | ABAQUS – FE 20 mm |                |                  | LTBeam | General<br>Formula<br>eq. (1) |
|---------------|-------------------|----------------|------------------|--------|-------------------------------|
|               | Solid FE<br>C3D20 | Shell FE<br>S4 | Beam FE<br>B32OS |        |                               |
| 4.5           | 33,03             | 32,75          | 33,38            | 33,19  | 33,64                         |
| 6.0           | 25,11             | 24,83          | 25,25            | 25,08  | 25,46                         |
| 7.5           | 20,41             | 20,15          | 20,46            | 20,32  | 20,65                         |

Finite elements in the C3D20 model have a non-linear shape function describing them which gives better results, for example, when the dimensions of the nodes are different. However, use of non-linear functions increases the computation time (a quadratic function requires three variables instead of 2, as in a linear function). Finite elements of the B32OS model are invulnerable to the changes in nodes geometry that model them because they are distributed along the element. This results in an inability to model a linear I-beam made out of ES B32OS strengthened with stiffeners (in another way, with varying cross-section). For the purpose of this study, the model B32OS is added only as a comparison for different types of discretization. As seen in Table 3, the results for a particular I-beam length are similar. This means that the boundary conditions and I-beams have been modelled properly in the ABAQUS environment.

Results have shown that a model computed with the use of S4 finite elements allows obtaining similar results to the one modelled with C3D20 elements. As it requires five times fewer operations, the following considerations will be based on this node type. As the computation time does not increase between the 30 mm and 20 mm nodes, a smaller mesh size was taken for further consideration.

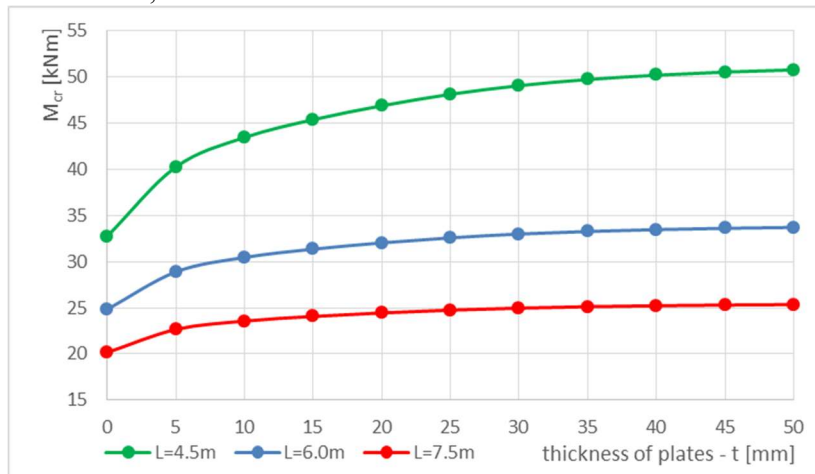


Fig. 5. Relationship between load and the largest lateral displacement of a top flange in the middle of the span for different load at the time of enhancement

The results presented in Figure 5 show the correlation between the critical moment value and bimoment restraints added to different I-beam sizes. Regardless of I-beam length, the highest increase in the critical moment can be seen when the first restraint is added to the model. The lower the I-beam length, the higher the percentile increase of the critical model caused by the installing of the restraints. The addition of the susceptible restraints shortens the length of warping to the

span between them. The shorter the beam, the higher the share of plate length in the total beam length.

#### 4.2. Determination of load-bearing capacity using the Finite Element Method

Figures 6-8 present the results of the calculations of the load-bearing capacity of I-beams ( $L=4.5$  m;  $6.0$  m;  $7.5$  m) obtained using FEM in ABAQUS software. The calculations used a non-linear material model (Figure 4) and initial equivalent imperfection [18]. The x-axis shows the thickness of plates used for bimoment strengthening. The thickness of the plates was the same on both sides of the beam and at both ends. For the thickness of  $0$  mm, the load-bearing capacity was calculated for the I-beam without additional strengthening plate. The red asymptote shows the load-bearing capacity for infinitely stiff plates.

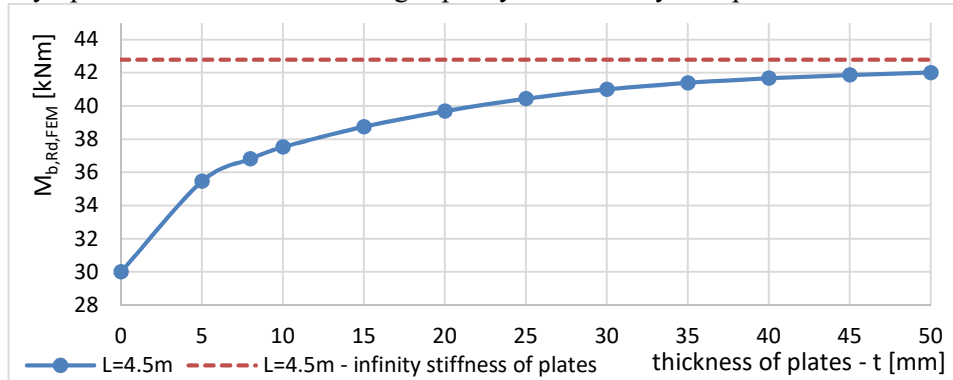


Fig. 6. Relationship between the load-bearing capacity of bending calculated in ABAQUS and the thickness of plates for bimoment stiffeners used in beam  $L=4.5$  m

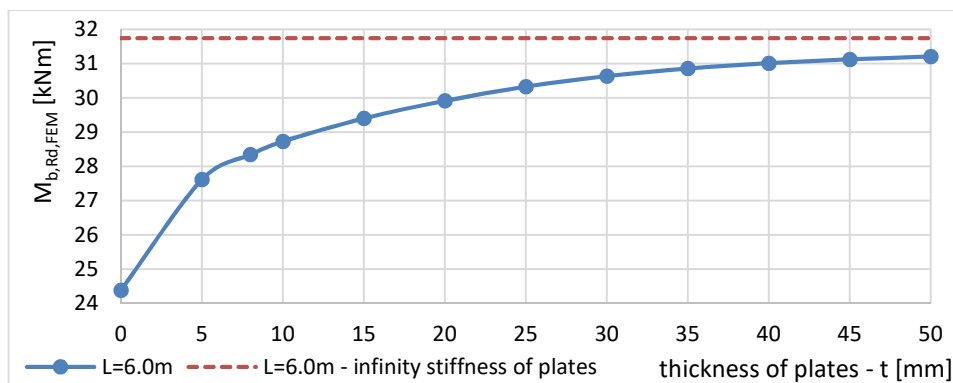


Fig. 7. Relationship between the load-bearing capacity of bending calculated in ABAQUS and the thickness of plates for bimoment stiffeners used in beam  $L=6.0$  m

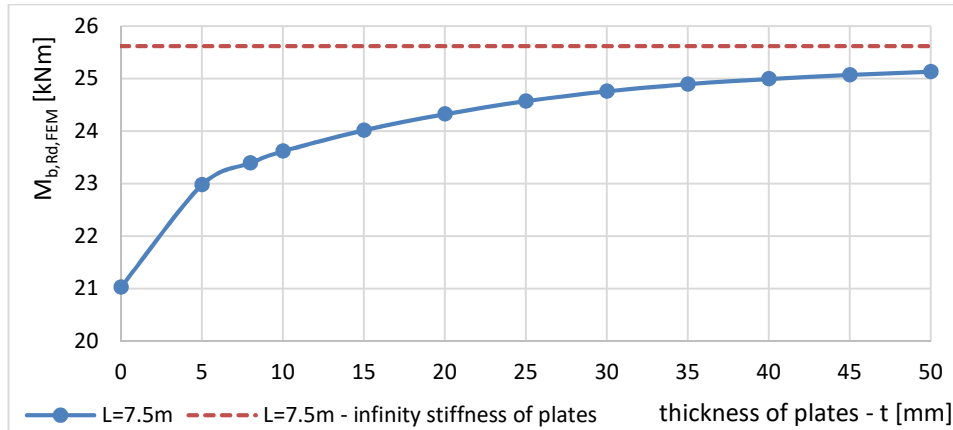


Fig. 8. Relationship between the load-bearing capacity of bending calculated in ABAQUS and the thickness of plates for bimoment stiffeners used in beam  $L=7.5$  m

As shown in Figures 6-8, implementation of strengthening plates with thickness of more than 30 mm allows obtaining near asymptotic values of load-bearing capacity. The largest increase in the values obtained in the study was seen between the beams without plates and plates with minimal thickness. The study did not analyse the load-bearing capacity of the plates themselves and their connection to the I-beam. In every case, the plastic load-bearing capacity was higher than the load-bearing capacity of bending with warping.

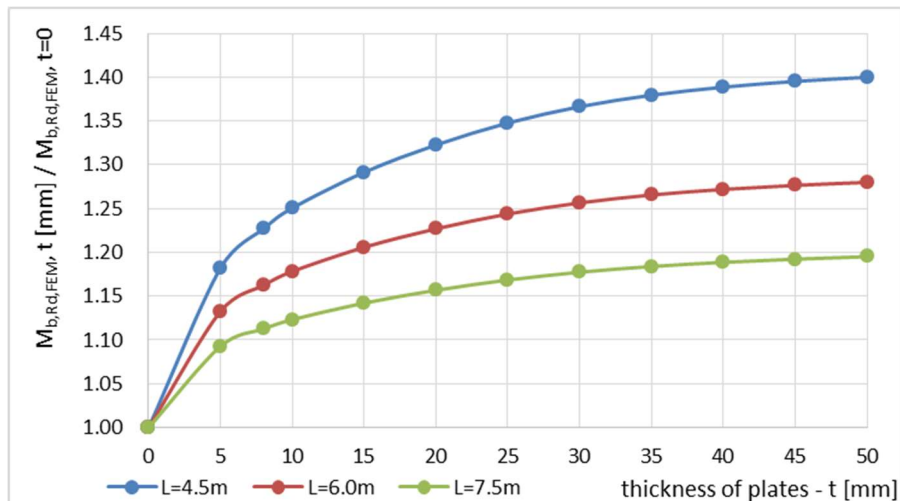


Fig. 9. The growth of load-bearing capacity of bending with LTB due to FEM according to thickness of bimoment stiffeners

Figure 9 proves that the bimoment restraints have a higher percentile influence on the load-bearing capacity of the shortest beams out of all studied beams. The longer the beam, the lower the influence of installed plates on the load-bearing capacity. Addition of even the thinnest plate, as in case of the critical moment, significantly increases the load-bearing capacity of the beam. Increase in the plate thickness above 30 mm does not significantly improve the load-bearing capacity.

## 5. SUMMARY AND CONCLUSIONS

This study analysed the influence of strengthening plates on the values of the critical moment and load-bearing capacity on the fork supported I-beam IPE200 (S355JR). Influence of different types of discretization on both the results and computation time have been analysed. The values of critical moment for the beam without the strengthening plates have been determined using FEM in ABAQUS and compared with results acquired in LTBeam software and formulas found in literature. A solution for determination of the load-bearing capacity with the use of GMNIA has been proposed. The solution assumes initial geometrical imperfections corresponding to the elastic lateral-torsional buckling. The load-bearing capacity has then been calculated for three different beams lengths and eleven different strengthening plate thicknesses as well as for a reference model without the restraints.

Based on the acquired results it can be said that the bimoment restraints significantly increase the value of the critical moment and load-bearing capacity of the beams. The shorter the beam, the higher the percentile increase of the load-bearing capacity. Use of short beams brings about the problem of loss of load-bearing capacity due to yield of the section, thus, in this study, the slenderness of the beams was assumed to prevent this occurrence (the chosen section was the IPE in class 1). As seen in the results, the effect of strengthening occurred after the implementation of even the thinnest plates (5 mm). The study does not regard the plates themselves and their connections. Plates are commonly used for load-bearing beams, mostly for strengthening the connections of the steel structure. However, their beneficial influence on the load-bearing capacity is often disregarded. Use of restraints with a thickness below 30 mm allows strengthening of the structure to a higher degree than the use of endplates, as the restraints have higher torsional stiffness in the warping plane. In the case of endplates their thickness has the most significance in increasing the load-bearing capacity of beams.

The author believes that it is possible to strengthen existing bent elements using plates, particularly the bimoment restraint, and will further develop this scientific topic.

## REFERENCES

1. EN 1993-1-1 “Eurocode 3 : Design of steel structures – Part 1-1 : General rules and rules for buildings”, CEN, 2006.
2. EN 1993-1-1 “Eurocode 3: Design of steel structures – Part 1-1 : General rules and rules for buildings”, CEN, 1992.
3. EN 1999-1-1 “Eurocode 9: Design of aluminium structures – Part 1-1: General structural rules, CEN 2007.
4. Galambos, TV and Surovek, AE 2008. Structural Stability of Steel: Concepts and Applications for Structural Engineers”, 236-289.
5. Gosowski, B 2015. Bending and torsion of thin walled metal structures (in Polish).
6. Badari, B and Papp, F 2015. On Design Method of Lateral-torsional Buckling of Beams: State of the Art and a New Proposal for a General Type Design Method. *Periodica Polytechnica Civil Engineering* **59(2)**, 179-192.
7. Rykaluk, K 2012. Stability issues of metal structures (in Polish), 176-201.
8. Szalai, J and Papp, F 2010. On the theoretical background of the generalization of Ayrton-Perry type resistance formulas. *Journal of Constructional Steel Research* **66**, 670-679.
9. Taras, A and Greiner, R 2010. New design curves for lateral-torsional buckling – Proposal based on consistent derivation. *Journal of Constructional Steel Research* **66**, 648-663.
10. Giżejowski, M, Szczerba, R and Gajewski, M 2016. FEM models and simulation methods in lateral-torsional buckling analysis of steel elements (in Polish). *JCEAA*, t. XXXIII, z.63 (1/I/16), 339-346.
11. Giżejowski, M, Szczerba, R and Gajewski, M 2017. Influence of imperfections on LTB resistance of steel rolled and welded beams (in Polish). *JCEAA*, t. XXXIV, z.64 (3/I/17), 447-460.
12. EN 10034, Structural steel I and H sections – Tolerances on shape and dimensions, CEN, Brussels, 1996.
13. PN-EN 1090-2, Wykonywanie konstrukcji stalowych i aluminiowych – Część 2: Wymagania techniczne dotyczące wykonania konstrukcji stalowych, PKN, Warszawa, 2014.
14. Wierzbicki, K 2018. Influence of endplates on the value of critical moment. 2018 International Interdisciplinary PhD Workshop (IIPhDW), 142-146.
15. Kurzawa, Z, Rzeszut, K, Szumigala, M and Chybinski, M 2006. Influence of endplates on the Critical Moment of I-beams (in Polish). *Inżynieria i Budownictwo* Nr **3/2006**, 163-166.
16. Piotrowski, R and Szychowski, A 2015. Lateral-torsional buckling of beams elastically restrained against warping at supports. *Archives of Civil*

- Engineering*, Vol. **LXI**, Issue 4, 155-174.
17. Iwicki, P 2010. Sensivity analysis of buckling loads of bisymmetric I-section columns with bracing elements. *Archives of Civil Engineering*, Vol. **LVI**, Issue 1, 69-88.
  18. Snijder, HH, RP van der Aa, B. W E. M. van Hove 2018. Lateral torsional buckling design imperfections for use in non-linear FEA. *Steel Construction: Design and Research* **11(1)**, 49-56.
  19. Vales, J and Stan, TC 2017. FEM Modelling of Lateral-Torsional Buckling using Shell and Solid Elements. *Procedia Engineering* **190**, 464-471.

*Editor received the manuscript: 18.02.2020*